Human CD141^{+} (BDCA-3)[+] dendritic cells (DCs) represent a unique myeloid DC subset that cross-presents necrotic cell antigens

Sarah L. Jongbloed,[1] Andrew J. Kassianos,[1,2] Kylie J. McDonald,[1] Georgina J. Clark,[1,2] Xinsheng Ju,[1] Catherine E. Angel,[3] Chun-Jen J. Chen,[3] P. Rod Dunbar,[3,4] Robert B. Wadley,[1] Varinder Jeet,[1] Annelie J.E. Vulink,[1] Derek N.J. Hart,[1,2,5] and Kristen J. Radford[1,2]

[1]Dendritic Cell Program, Mater Medical Research Institute, South Brisbane, Queensland 4101, Australia
[2]University of Queensland Faculty of Health Sciences, Herston, Queensland 4029, Australia
[3]School of Biological Sciences and [4]Maurice Wilkins Centre for Molecular Biodiscovery, University of Auckland, Auckland 1142, New Zealand
[5]Cooperative Research Centre for Biomarker Translation, La Trobe University, Bundoora, Victoria 3086, Australia

The characterization of human dendritic cell (DC) subsets is essential for the design of new vaccines. We report the first detailed functional analysis of the human CD141^{+} DC subset. CD141^{+} DCs are found in human lymph nodes, bone marrow, tonsil, and blood, and the latter proved to be the best source of highly purified cells for functional analysis. They are characterized by high expression of toll-like receptor 3, production of IL-12p70 and IFN-β, and superior capacity to induce T helper 1 cell responses, when compared with the more commonly studied CD1c^{+} DC subset. Polyinosine-polycytidylic acid (poly I:C)–activated CD141^{+} DCs have a superior capacity to cross-present soluble protein antigen (Ag) to CD8^{+} cytotoxic T lymphocytes than poly I:C–activated CD1c^{+} DCs. Importantly, CD141^{+} DCs, but not CD1c^{+} DCs, were endowed with the capacity to cross-present viral Ag after their uptake of necrotic virus-infected cells. These findings establish the CD141^{+} DC subset as an important functionally distinct human DC subtype with characteristics similar to those of the mouse CD8α^{+} DC subset. The data demonstrate a role for CD141^{+} DCs in the induction of cytotoxic T lymphocyte responses and suggest that they may be the most relevant targets for vaccination against cancers, viruses, and other pathogens.

CORRESPONDENCE
Kristen J. Radford:
kradford@mmri.mater.org.au

Abbreviations used: Ab, antibody; Ag, antigen; HCMV, human CMV; MoDC, monocyte-derived DC; poly I:C, polyinosine-polycytidylic acid; TLR, toll-like receptor; *TYROBP, TYRO protein tyrosine binding protein*; UBC, ubiquitin C; UCE, ubiquitin-conjugating enzyme.

The essential role of DCs in the induction and regulation of immune responses to pathogens, self-antigens (Ags), and cancers is now well established. All DCs excel at processing and presenting Ag and priming naive T cell responses, but the complexity of DC subsets and their individual specialized functions is just becoming apparent (MacDonald et al., 2002; Villadangos and Schnorrer, 2007; Naik, 2008). Promising DC-based therapeutic vaccines have been described to treat malignancies and infections (Vulink et al., 2008), but the majority of these use in vitro–generated monocyte-derived DC (MoDC), and the physiological standing of this DC subtype is currently unclear. Understanding the emerging complexities of human DC subset biology is therefore essential to develop new vaccines and therapeutics targeting DC.

The characterization and function of human DC subsets has been confounded by their rarity, the lack of distinctive markers, and limited access to human tissues. Human blood DCs comprise ~1% of circulating PBMCs and have been classically defined as Ag-presenting leukocytes that lack other leukocyte lineage markers (CD3, 14, 15, 19, 20, and 56) and express high levels of MHC class II (HLA-DR) molecules (Hart, 1997). These can be broadly categorized into two groups: plasmacytoid

S.L. Jongbloed and A.J. Kassianos contributed equally to this paper.
D.N.J. Hart and K.J. Radford contributed equally to this paper.
D.N.J. Hart's present address is ANZAC Research Institute, Concord Hospital, Sydney NSW 2139, Australia.
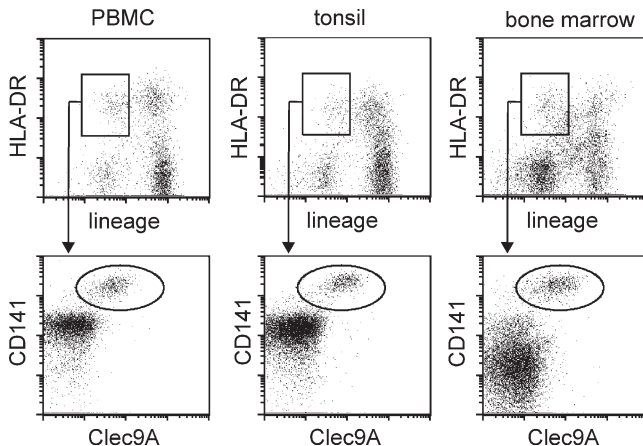
Figure 1. CD141+ DCs are located in human tonsil, bone marrow, and peripheral blood. DCs in human peripheral blood (PBMC), tonsil, and bone marrow were identified as lineage−HLA-DR+ events (top), and CD141+CLEC9A+ cells within this population are shown (bottom). The percentage of total mononuclear cells that were CD141+CLEC9A+ for the donor illustrated was 0.05% in PBMC, 0.08% in tonsil, and 0.05% in bone marrow. Analysis of one of three donors for each tissue is shown.

CD11c−CD123+ DC and conventional or myeloid CD11c+CD123− DC. We have described three further phenotypically distinct subsets of CD11c+ DC, defined by their expression of CD16, CD1c (BDCA-1), and CD141 (BDCA-3; MacDonald et al., 2002). Gene expression profiling and hierarchical clustering data has indicated that plasmacytoid DC and CD16+ DC arise from separate precursor

cells, whereas the CD1c+ DC and CD141+ DC subsets appear to have a common origin and represent two different stages of a similar subset (Lindstedt et al., 2005). However, CD1c+ and CD141+ DCs each have unique gene expression profiles distinct from monocytes and MoDC, and this predicts that they have different functions (Dzionek et al., 2000; MacDonald et al., 2002; Lindstedt et al., 2005).

The concept of distinct DC subtypes with unique capabilities to influence immunological outcomes is exemplified by the mouse CD8α− and CD8α+ conventional DC subsets that reside in the lymph nodes and spleen (Villadangos and Schnorrer, 2007; Naik, 2008). The CD8α− DC subset appears to be most effective at inducing Th2 responses (Maldonado-López et al., 1999; Pulendran et al., 1999) and processing and presenting Ag to CD4+ T cells via the MHC class II pathway (Pooley et al., 2001; Dudziak et al., 2007; Villadangos and Schnorrer, 2007). In contrast, the CD8α+ DC subset has a unique ability to take up dead or dying cells and to process and present exogenous Ag on MHC class I molecules to CD8+ T cells (i.e., cross-presentation; den Haan et al., 2000; Iyoda et al., 2002; Schnorrer et al., 2006). There is now substantial evidence that the CD8α+ DC subset plays a crucial role in the induction of protective CD8+ CTL responses that are essential for the eradication of cancers, viruses, and other pathogenic infections (Dudziak et al., 2007; Hildner et al., 2008; López-Bravo and Ardavín, 2008; Naik, 2008). The identification of the human DC subset with similar functional capacity would be a significant advance and would enable translation of mouse DC biology into clinical practice.

Correlation of the human and mouse DC subsets has been hampered by differences in their defining markers (human DCs do not express CD8α). Interestingly, computational genome-wide expression profiling clustered human CD141+ DC and CD1c+ DC with the mouse CD8α+ and CD8α− conventional DC subsets, respectively (Robbins et al., 2008). Human CD141+ DC and mouse CD8α+ DC share a number of phenotypic similarities,
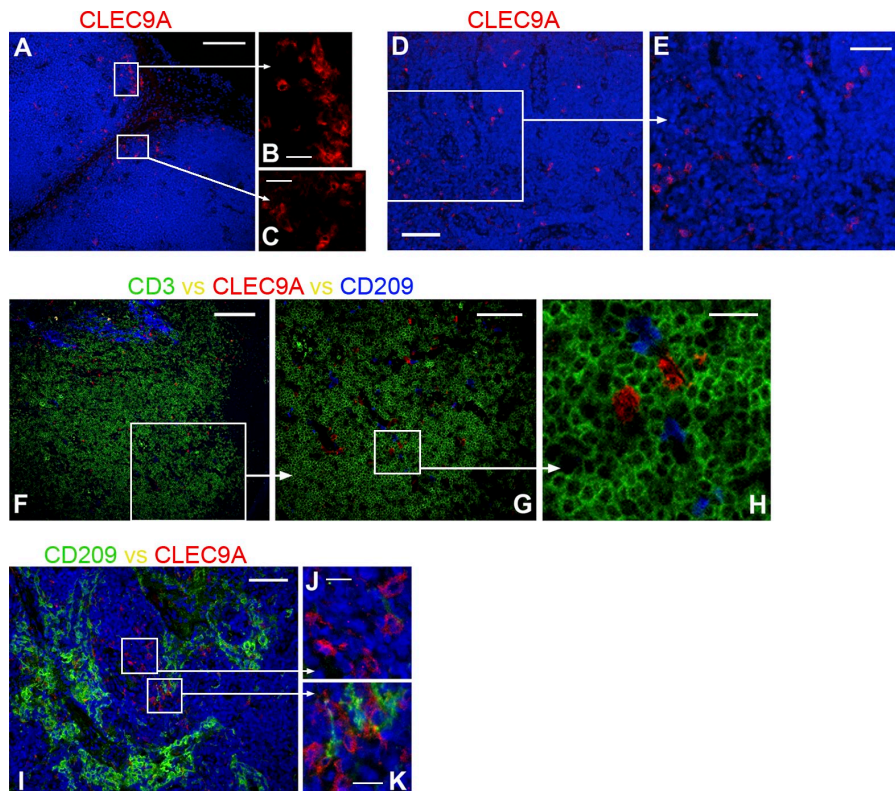

Figure 2. CD141+ DCs are located in human lymph nodes. Cells expressing CLEC9A in human lymph nodes colonized the paracortex beneath the capsule and trabeculae (A–C), the more central areas of the CD3+ T cell rich paracortex (D–H), and the diffuse paracortex that protrudes between the medullary cords (I–K). Co-staining with CD209 demonstrated that neither the CD209+ antigen-presenting cells in the medullary cords nor the surrounding diffuse paracortex expressed CLEC9A (F–K). Blue represents DAPI staining of cell nuclei (A, D, E, I, J, and K). Bars: (A and F) 200 µm; (D, G, and I) 100 µm; (E) 50 µm; (B and C) 30 µm; (H, J, and K) 20 µm.
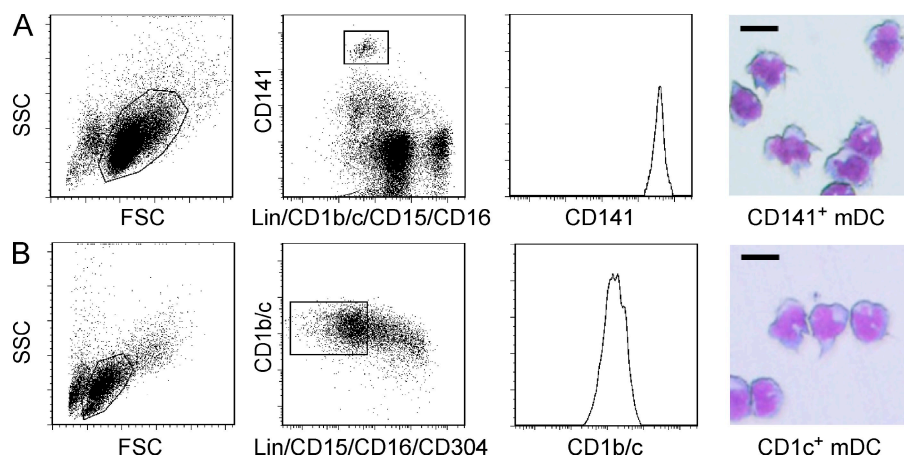
The function of human CD141+ dendritic cells | Jongbloed et al.

Figure 3. Isolation of CD141+ DC and CD1c+ DC from apheresis products. (A) CD141+ DCs were enriched by an initial immunomagnetic depletion of lin+ cells and sorted as CD141^{bright} lin−CD1c−CD15−CD16−. (B) CD1c+ DCs were first enriched using a BDCA-1 immunomagnetic selection kit and further purified by flow cytometry sorting to remove residual contaminating cells. Morphology of purified DC is shown at 100× magnification. Bars, 10 µm.

including expression of Toll-like receptor (TLR) 3 (Edwards et al., 2003; Lindstedt et al., 2005), the novel surface molecule Necl2 (nectin-like protein 2; Galibert et al., 2005), and the C-type lectin CLEC9A (Caminschi et al., 2008; Huysamen et al., 2008; Sancho et al., 2008). Thus, whether the human CD141+ DC subset is the human functional equivalent of the mouse CD8α+ DC subset has now become a major question for immunologists.

CD141+ DCs constitute only ∼0.03% of human PBMCs and, although present in other human tissues, their low proportions and difficulties with aseptic human tissue access mean that they have never been isolated in sufficient quantity to study their function until now. We report the first detailed functional analysis of human CD141+ DCs in response to TLR3 stimuli and define their role in the induction of Th1 responses and cross-presentation.

RESULTS

CD141+ DCs reside in blood and lymphoid tissues

The C-type lectin CLEC9A is selectively expressed by human CD141+ DC (Caminschi et al., 2008; Huysamen et al., 2008; Sancho et al., 2008). We confirmed CLEC9A expression on blood CD141+ DC and identified CD141+CLEC9A+ cells in human tonsils and bone marrow (Fig. 1). The CD141+CLEC9A+ DC comprised from 0.03 to 0.08% of the total mononuclear cells in these tissues. We then stained human lymph nodes and identified CLEC9A+ cells with morphology suggestive of DC (Fig. 2, A–E). These cells were distributed throughout the CD3+ T cell–rich paracortex (Fig. 2, A–H), including the diffuse T cell areas adjacent to the medullary cords (Fig. 2, F and I–K). CD209 defines a population of lymph node–resident Ag-presenting cells that colonizes the medullary cords and paracortex (Angel et al., 2009) but is not expressed by blood DC (MacDonald et al., 2002). Co-staining with CLEC9A and CD209 antibody (Ab) showed that all the CLEC9A+ cells were CD209− and, although occasional CLEC9A+ cells were present in the medullary cords, the vast majority of CLEC9A+ cells were restricted to paracortical areas (Fig. 2, F–K). Thus, CLEC9A+ DCs represent a lymph node paracortical DC population that is distinct from the CD209+ population.
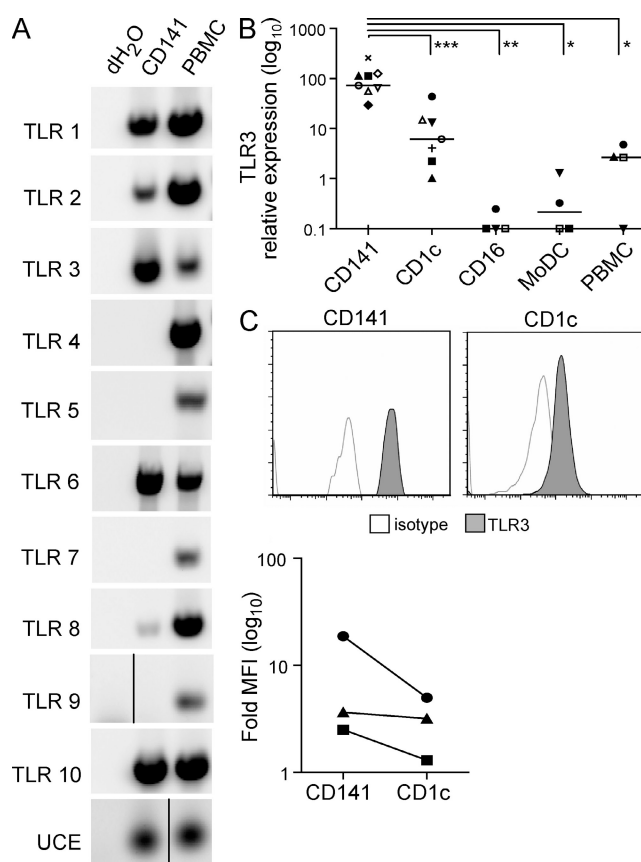

Figure 4. CD141+ DCs express high levels of TLR3. (A) TLR1-10 mRNA expression by purified CD141+ DC and autologous PMBC by PCR. Data are representative of three donors for TLR9 and four donors for all other TLR, with the exception that TLR7 expression was found in one of four donors. Black lines indicate that intervening lanes have been spliced out. (B) TLR3 expression on human myeloid DC subsets determined by quantitative PCR relative to ubiquitin-conjugating enzyme (UCE). *, P = 0.03; **, P = 0.02; ***, P = 0.01. Symbols represent DC isolated concurrently from the same donor. (C) TLR3 expression by fluorescent intracellular staining of CD141+ DC and autologous CD1c+ DC. Top, histograms from a representative donor. Bottom, fold increase in mean fluorescence intensity (MFI) of TLR3 over the isotype control for three donors.
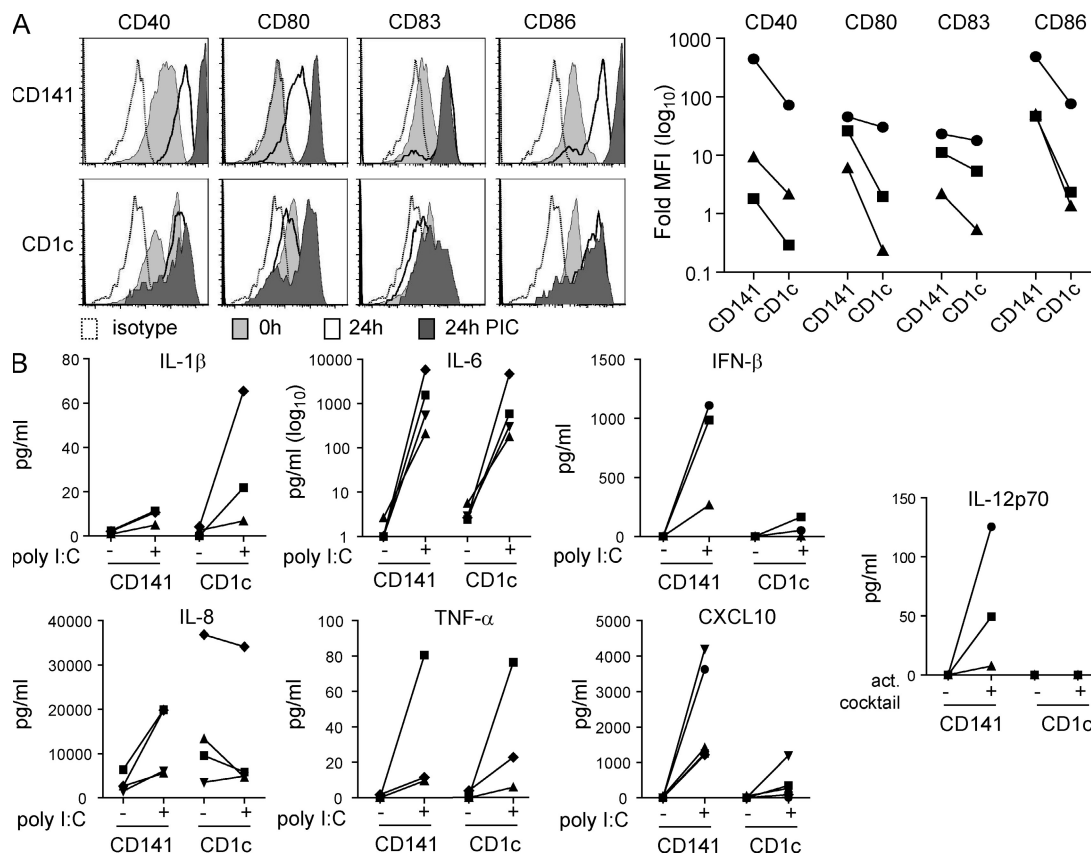
1249

Figure 5. CD141+ DCs secrete IFN–β, CXCL10, and IL–12p70. (A) Expression of costimulatory molecules CD40, CD80, CD83, and CD86 by CD141+ DC and autologous CD1c+ DC freshly isolated (0 h) or after 24-h culture in complete medium alone (24 h) or in the presence of poly I:C (24 h PIC). Left, one example of three donors is shown in histograms. Right, CD141+ DCs express higher levels of costimulatory markers after activation with poly I:C compared with autologous CD1c+ DCs. The fold increase in the MFI over the isotype control for three donors is shown. (B) Secretion of inflammatory cytokines and chemokines by CD141+ DC and autologous CD1c+ DC after stimulation with poly I:C and secretion of IL-12p70 after activation with a cocktail of poly I:C, IFN-γ, TNF, IFN-α, and IL-1β.

CD141+ DCs express high levels of TLR3 and produce IFN–β and IL–12p70

Because PBMCs are the most feasible source of CD141+ DC, we developed a protocol to isolate highly pure (>99%) CD141+ DC from healthy donor leukapheresis products in sufficient numbers for phenotypic and functional analyses. This procedure consisted of an initial depletion of lineage-positive mononuclear cells by negative immunomagnetic selection followed by flow cytometry sorting for CD141+ DC (Fig. 3 A). Consistent with their low frequency, we obtained, on average, 100 ($\pm$ SD 45, $n = 17$) highly pure CD141+ DCs per 10^6 input PBMCs. CD1c+ DCs were isolated by first depleting B cells and enriching for CD1c+ DCs using a commercial immunomagnetic selection kit and then further purified by flow cytometry sorting (Fig. 3 B). Consistent with their higher abundance in blood, the yields of CD1c+ DCs were significantly higher (1,023 $\pm$ 683, mean $\pm$ SD) per 10^6 input PBMCs ($n = 17$; P < 0.0001 by paired two-tailed Student's t test compared with autologous CD141+ DCs). DC isolation and analysis was more challenging on tonsil tissue, but there was a greater percentage of CD141+ than

CD1c+ cells in tonsil mononuclear cells (unpublished data). Both subsets isolated from blood exhibited similar morphology and phenotype to those previously described (Dzionek et al., 2000; MacDonald et al., 2002; Fig. 3 and not depicted). We also examined the transcription factors *IRF8* and *Batf3*, which are essential for mouse CD8α+ DC differentiation (Fig. S1; Schiavoni et al., 2002; Aliberti et al., 2003; Hildner et al., 2008). We found no differences in their expression between CD141+ DC and autologous CD1c+ DC. In mice, *IRF8* positively regulates *indoleamine 2,3-dioxygenase* (*IDO*) transcription but negatively regulates *TYRO protein tyrosine binding protein* (*TYROBP*), which encodes signaling adapter DAP12. Thus, *IRF8* expression is associated with a tolerogenic phenotype and *TYROBP* expression with an immunogenic phenotype (Orabona et al., 2006). Consistent with mouse CD8α+ DC and human gene expression profiling data (Robbins et al., 2008), we found that the *IRF8/TYROBP* mRNA ratio was higher in freshly isolated CD141+ DC than in autologous CD1c+ DC in four or five donors (Fig. S1).

To gain insight into CD141+ DC function, we first examined its TLR expression profile. CD141+ DC expressed
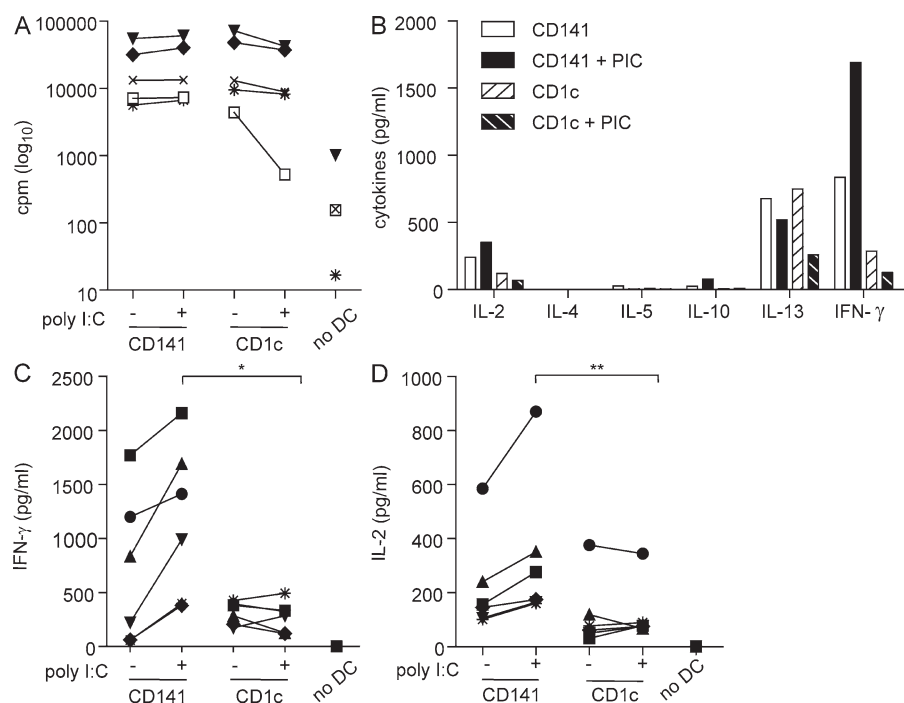
Figure 6. Poly I:C–activated CD141+ DCs induce superior CD4+ Th1 responses compared with CD1c+ DCs in an allogeneic MLR. (A) Allogeneic CD4+ T cell proliferation induced by unstimulated (−) or poly I:C activated (+) CD141+ DC and autologous CD1c+ DC, or in the absence of DC (no DC), measured by ^{3}[H]-thymidine incorporation and expressed as counts per minute (cpm) after 6 d. (B) Cytokine production in the MLR cultures after 6 d. One representative donor of six is shown. (C and D) Secretion of IFN-γ (C) and IL-2 (D) in the allogeneic MLR cultures after 6 d. Each symbol represents DC isolated from the same donor in all graphs. *, P = 0.063; **, P = 0.031.

CD1c+ DC produced higher levels of IL-1β than CD141+ DC, whereas similar levels of IL-6, IL-8, and TNF were produced by both subsets (Fig. 5 B). Neither subset produced detectable levels of IL-10 (unpublished data). TLR3 triggering induces the production of IFN-β, which is known to enhance Th1 responses and cross-priming (Schulz et al., 2005; Le Bon and Tough, 2008). When activated with poly I:C, CD141+ DC secreted substantially more IFN-β protein than CD1c+ DC (Fig. 5 B). Neither subset produced detectable IFN-α mRNA (unpublished data). The chemokine CXCL10 (IP-10), which plays an important role in the generation of antiviral immunity (Rudd et al., 2005; Lindell et al., 2008), was also produced in higher levels by CD141+ DC than by CD1c+ DC in response to poly I:C (Fig. 5 B). IL-12p35 mRNA expression was induced in poly I:C–activated CD141+ DC, but this was not enhanced by the addition of CD40L, and IL-12p70 protein was undetectable in the culture supernatants (unpublished data). Autologous CD1c+ DC expressed minimal or no IL-12p35 mRNA or IL-12p70 protein under the same conditions (unpublished data). However, CD141+ DC, but not CD1c+ DC, did produce IL-12p70 when stimulated with a cocktail of poly I:C, IFN-γ, TNF, IFN-α, and IL-1β (Fig. 5 B). The significantly higher expression of TLR3 by CD141+ DCs and their capacity to produce IFN-β, CXCL10, and IL-12p70 are consistent with a Th1-inducing function.

CD141+ DCs induce superior Th1 responses compared with CD1c+ DCs

The ability to induce proliferation of allogeneic CD4+ T cells in an MLR is one of the definitive features of DC. Therefore, we compared the ability of unstimulated and poly I:C–activated CD141+ DC and CD1c+ DC to induce CD4+ T cell responses in an allogeneic MLR. Both DC subsets were powerful and equivalent stimulators of allogeneic CD4+ T cell proliferation, regardless of their activation status (Fig. 6 A). Both subsets induced production of substantial levels of the Th1

mRNA for TLR1, 2, 3, 6, 8, and 10 but lacked expression of TLR4, 5, 7, and 9 (Fig. 4 A). This profile was similar to that of CD1c+ DC, with the exception that CD1c+ DC also expressed TLR4, 5, and 7 (Fig. S2). Notably, TLR3 was expressed by both CD141+ DC and CD1c+ DC and is also expressed by MoDC (Fig. S2; Kadowaki et al., 2001; Matsumoto et al., 2003; Lindstedt et al., 2005), which contrasts with the selective expression of TLR3 by CD141+ DC which is predicted by gene expression profiling (Lindstedt et al., 2005; Robbins et al., 2008). To reconcile this, we quantitated TLR3 mRNA expression by RT-PCR in purified human myeloid DC subsets and confirmed TLR3 expression by CD141+ DC, CD1c+ DC, and MoDC but not CD16+ DC (Fig. 4 B). However, the relative expression of TLR3 mRNA was significantly higher on CD141+ DC than on CD1c+ DC and MoDC (Fig. 4 B), and increased TLR3 protein expression was confirmed by intracellular staining (Fig. 4 C). These data demonstrate that CD141+ DCs are the major human DC subset expressing TLR3.

We next compared the ability of CD141+ DC and autologous CD1c+ DC to respond to the TLR3 agonist polyinosine-polycytidylic acid (poly I:C). Poly I:C did not markedly affect the viability of either cell type (unpublished data). Freshly isolated CD141+ and CD1c+ DC expressed CD40 and CD86 with no or low CD80 and CD83 as previously reported (Dzionek et al., 2000; MacDonald et al., 2002; Fig. 5 A). Overnight incubation in culture medium alone up-regulated costimulatory molecule expression on both populations, whereas poly I:C stimulation up-regulated costimulatory molecule expression to a greater extent on CD141+ DC than on CD1c+ DC (Fig. 5 A). Stimulation with poly I:C induced production of inflammatory cytokines by both CD141+ DC and CD1c+ DC.

1251

cytokine IFN-γ by the T cell cultures (Fig. 6 B). IFN-γ was not detected in the supernatants of DC cultured alone (not depicted) or T cells cultured in the absence of DC (Fig. 6 C). CD141⁺ DC and CD1c⁺ DC also induced production of IL-2, whereas there was little or no production of the Th2 cytokines IL-4 and IL-5 and the regulatory cytokine IL-10 (Fig. 6 B). RORγt mRNA (a measure of Th17 induction) and FoxP3 mRNA (a measure of regulatory T cells) were undetectable in the cultures (unpublished data). Both subsets induced production of IL-13 that, although commonly associated with Th2 responses, can also be associated with high IFN-γ–producing Th1 responses in cancer and infectious diseases (Alexander and McFarlane, 2008; Kyte et al., 2009). Notably, CD141⁺ DC stimulated secretion of higher levels of IFN-γ and IL-2 by T cells compared with CD1c⁺ DC that was further enhanced after poly I:C activation (Fig. 6, C and D). These data demonstrate that CD141⁺ DCs are strong inducers of Th1 responses.

CD141⁺ DCs process and present recombinant protein to CD4⁺ T cells

We examined whether CD141⁺ DC could take up, process, and present recombinant protein Ag to autologous CD4⁺ T cells. Freshly isolated CD1c⁺ DC expressed higher levels of mRNA encoding for Ifi30 (GILT), HLA-DMA, and Cathepsin H, which are reputedly associated with MHC class II processing (Dudziak et al., 2007; Fig. 7 A). However, CD141⁺ DC from three out of four donors expressed higher levels of HLA-DR compared with CD1c⁺ DC ex vivo (Fig. 7 A), and this was only marginally up-regulated by both subsets after overnight culture in medium alone or in the presence of poly I:C (Fig. 7, A and B). Both CD141⁺ and CD1c⁺ DC subsets had a similar capacity to take up Lucifer yellow (Fig. 7 C). To assess the capacity of the DC subsets to process and present recombinant soluble protein to CD4⁺ T cells, we used the human CMV (HCMV) pp65 matrix protein as a model Ag. HCMV establishes latency and persistency in healthy individuals that is associated in sero-positive donors with a high frequency of pp65-specific CD4⁺ and CD8⁺ T cells across multiple MHC alleles (Wills et al., 1996). CD141⁺ DC and CD1c⁺ DC from HCMV sero-positive donors could process and present recombinant pp65 to autologous CD4⁺ T cells with similar efficiency ex vivo in an IFN-γ production assay (Fig. 7 D).
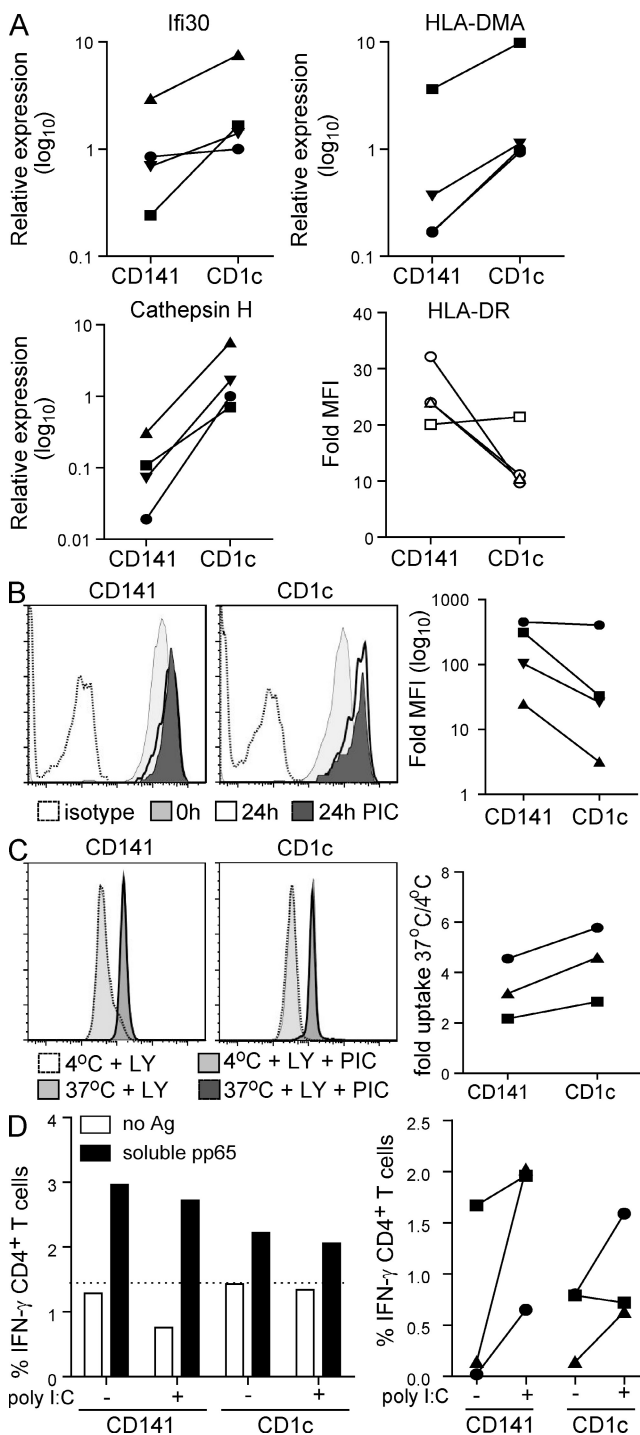
Figure 7. MHC class II processing and presentation of HCMV pp65 recombinant protein. (A) CD1c⁺ DCs express higher mRNA levels of MHC class II–associated molecules Ifi30, HLA-DMA, and Cathepsin H than autologous CD141⁺ DCs by quantitative PCR relative to ubiquitin C (UBC) in four donors. Surface expression of HLA-DR was measured by flow cytometry and expressed as the fold increase of MFI over isotype control. (B) Expression of HLA-DR on CD141⁺ DC and autologous CD1c⁺ DC freshly isolated (0 h) or after 24-h culture in complete medium alone (24 h) or in the presence of poly I:C (24 h PIC) in an example donor (histograms) and all three donors after poly I:C activation (right). (C) Lucifer yellow (LY) uptake by CD141⁺ DC and CD1c⁺ DC in the absence or presence of poly I:C (+ PIC) after 1 h of incubation at 4 or 37°C. One example donor is shown in the histograms, and LY uptake by three donors comparing the fold uptake at 37 over 4°C is shown on the right. (D) Processing and presentation of HCMV pp65 protein to CD4⁺ T cells by unstimulated (−) or poly I:C–activated (+) DC isolated from HCMV seropositive donors, as measured by intracellular IFN-γ production by autologous CD4⁺ T cells. The dotted line represents the maximum background IFN-γ production in the absence of pp65 (no Ag). One example donor is shown on the left and specific IFN-γ production (pp65-no Ag) for all three donors is shown on the right.
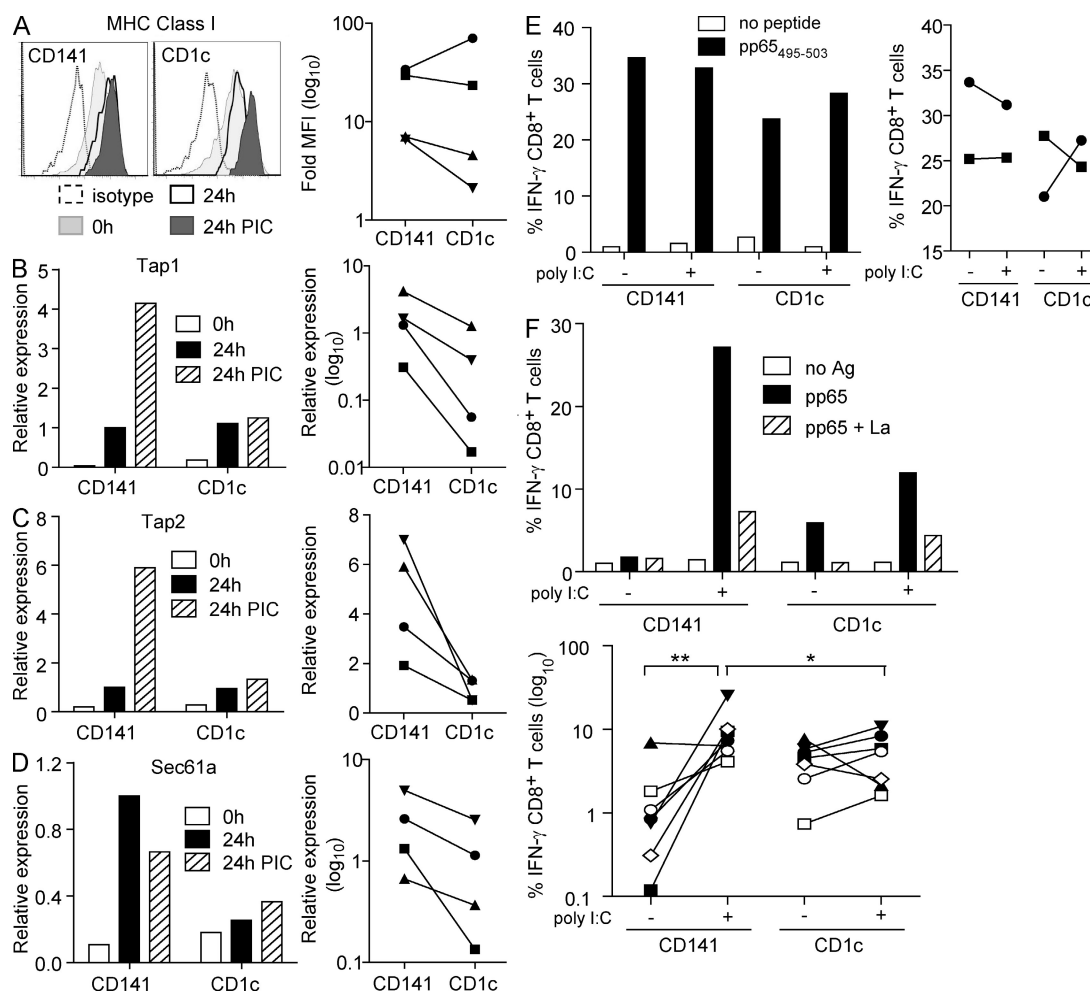
Figure 8.   Poly I:C stimulation of CD141+ DC enhances cross-presentation of HCMV pp65 recombinant protein. (A) Expression of MHC class I on CD141+ DC and autologous CD1c+ DC freshly isolated (0 h) or after 24-h culture in complete medium alone (24 h) or in the presence of poly I:C (24 h PIC). One representative is shown in the histograms, and MFI fold increase of MHC class I expression over the isotype control for four donors after activation with poly I:C is shown on the right. (B–D) Expression of Tap1 (B), Tap2 (C), and Sec61a (D) by CD141+ DC and autologous CD1c+ DC. One example donor is shown on the left and four donors after poly I:C activation is shown on the right. (E) Presentation of the pp65$_{495-503}$ peptide by CD141+ DC and CD1c+ DC from HLA-A*0201+ donors to a pp65$_{495-503}$–specific CD8+ T cell line. One representative donor (left) and specific IFN-γ production (pp65$_{495-503}$, no peptide) from two donors (right) is shown. (F) Cross-presentation of pp65 recombinant protein by CD141+ DC and autologous CD1c+ DC. Top, uptake of pp65 protein by DC subsets from a HLA-A*0201+ HCMV sero-negative donor and processing and presentation of the pp65$_{495-503}$ epitope to pp65$_{495-503}$–specific CD8+ T cells, as measured by T cell IFN-γ secretion. One example donor is shown. Cross-presentation is proteasome dependent, as it is inhibited by lactacystin (pp65 + La, one of three experiments). Bottom, specific IFN-γ production (pp65-noAg) by a pp65$_{495-503}$–specific CD8+ T cell line (using DC from HLA-A*0201+ donors; black) or CD8+ T cells (using autologous DC from HLA-A*0201− HCMV sero-positive donors; white) as responders. *, P = 0.047; **, P = 0.031.

Poly I:C enhances CD141+ DC cross-presentation of recombinant pp65 protein to CD8+ T cells

We investigated the ability of CD141+ DC to stimulate CD8+ T cells. Both CD141+ DC and CD1c+ DC expressed similar levels of MHC class I on their surface that was marginally up-regulated after overnight culture in medium alone or with poly I:C (Fig. 8 A). We then examined the expression of MHC class I processing pathway-associated molecules by CD141+ DC. Freshly isolated CD141+ DC and CD1c+ DC expressed similar low mRNA levels of Tap1 and Tap2 and Sec61a (Fig. 8, B–D). Although both subsets up-regulated

mRNA expression of Tap1, Tap2, and Sec61a after culture alone or in the presence of poly I:C, higher levels were induced by CD141+ DC than by CD1c+ DC when activated with poly I:C (Fig. 8, B–D).

To examine the capacity of CD141+ DC to directly present peptide Ag to CD8+ T cells, DCs from HLA-A*0201+ donors were pulsed with the HLA-A*0201-restricted HCMV pp65$_{495-503}$ peptide in the absence or presence of poly I:C and used to stimulate a pp65$_{495-503}$-specific CTL line. As suggested by their level of MHC class I expression, CD141+ DCs were effective and comparable to autologous CD1c+ DCs in their

presentation of peptide Ag to CD8^{+} T cells, and this was not enhanced by poly I:C (Fig. 8 E).

Cross-presentation is the process by which acquired exogenous Ag can gain access to the MHC class I processing pathway of DC to elicit CD8^{+} CTL responses. This is enhanced by TLR3 triggering (Schulz et al., 2005) and IFN-β (Le Bon and Tough, 2008). The high expression of TLR3 by CD141^{+} DCs and their ability to produce IFN-β after stimulation with poly I:C are consistent with a specialized role in cross-presentation. We therefore assessed the capacity of CD141^{+} DC to process and present HCMV pp65 recombinant protein to responding CD8^{+} T cells. Specific processing and presentation of the pp65$_{495-503}$ epitope, after uptake of pp65 protein by HLA-A*0201^{+} DC from HCMV sero–negative donors, was examined by stimulation of a pp65$_{495-503}$–specific CD8^{+} T cell line. HCMV sero-positive donors expressing different HLA alleles were also used to test processing and presentation of pp65 using a single ex vivo stimulation of autologous CD8^{+} T cells. Similar findings were obtained using both assays (Fig. 8 F). In most donors, CD141^{+} DCs were inefficient at cross-presenting unless activated with poly I:C, whereas CD1c^{+} cross-presented even in the absence of activation (Fig. 8 F). Importantly, CD141^{+} DCs were more effective at cross-presentation on a per cell basis than autologous CD1c^{+} DCs after poly I:C activation (Fig. 8 F). Activation with LPS did not enhance the capacity of CD1c^{+} DC to cross-present compared with poly I:C or unstimulated CD1c^{+} DC (Fig. S3 C). Processing of pp65 recombinant protein by CD141^{+} DC was confirmed to be proteasome dependent, as it was blocked by the proteasome inhibitor lactacystin (Fig. 8 F). Thus, although both DC subsets could cross-present recombinant protein, only cross-presentation by CD141^{+} DC was significantly enhanced by poly I:C.

CD141^{+} DCs cross–present Ag from HCMV–infected necrotic cells

Double stranded (ds) RNA released from dying cells and the dsRNA replication intermediary of many viruses are the natural ligands for TLR3 (Karikó et al., 2004; Cavassani et al., 2008). CLEC9A also acts as a sensor of necrotic cells and regulator of cross-priming in mice (Sancho et al., 2009). The superior capacity of CD141^{+} DCs to cross-present after TLR3 stimulation and their selective expression of CLEC9A imply a specialized role for CD141^{+} DC in the cross-presentation of Ag from dead or dying cells. This would be especially relevant for the generation of protective CTL responses against tumors and viruses that infect cells other than DC. We therefore investigated the ability of CD141^{+} DC to take up and cross-present Ag from HCMV-infected necrotic fibroblasts compared with autologous CD1c^{+} DC. For these experiments, the laboratory HCMV AD169 strain, which does not directly infect blood DC (Fig. S4), was used to infect HLA-A*0201^{−} fibroblasts, and secondary necrosis was induced by UV irradiation. This established a model in which processing and presentation of the pp65$_{495-503}$ epitope from HCMV could only occur via cross-presentation after uptake of the HCMV-infected

necrotic fibroblasts by HLA-A*0201^{+} DC. We first established that CD141^{+} DC and CD1c^{+} DC were similar in their capacity to ingest material from HCMV-infected necrotic fibroblasts (Fig. 9, A and B). Despite this, only CD141^{+} DC cross-presented the pp65$_{495-503}$ epitope after uptake of the HCMV-infected necrotic cells (Fig. 9 C). This demonstrated the specialized capacity of CD141^{+} DC to cross-present Ag from necrotic cells.

DISCUSSION

Our study is the first detailed functional analysis of the human CD141^{+} DC subset. We showed that, in contrast to human blood CD1c^{+} DC, the CD141^{+} DC subset expressed high levels of TLR3, but not TLR4, 5, or 7, and produced IFN-β, CXCL10, and IL-12p70. Poly I:C–activated CD141^{+} DC induced superior Th1 responses to those induced by CD1c^{+}
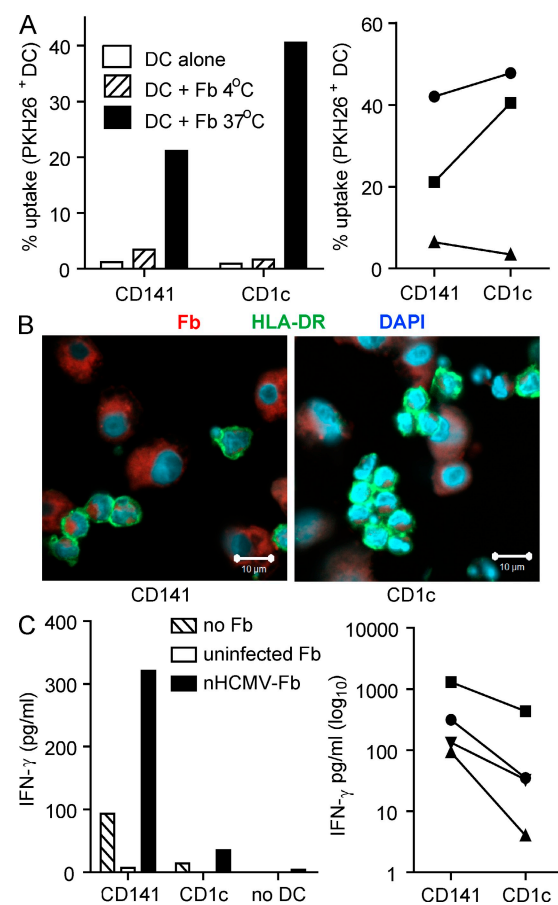

Figure 9. CD141^{+} DCs cross–present Ag from HCMV–infected necrotic fibroblasts. (A) Uptake of PKH-26–labeled HCMV-infected necrotic fibroblasts (nHCMV-Fb) by DC subsets after 12 h at 4 and 37°C by flow cytometry from a representative donor (left) and by three donors (right). (B) Uptake of nHCMV-Fb by confocal microscopy at 200×. Bars, 10 µm. (C) Cross-presentation of the pp65$_{95-503}$ epitope after uptake of nHCMV-Fb or control uninfected Fb by CD141^{+} DC and CD1c^{+} DC subsets to a pp65-specific CD8^{+} T cell line, as assessed by IFN-γ secretion by the T cells. Left, one representative of four donors. Right, four donors, expressed as specific IFN-γ production (nHCMV-Fb−uninfected Fb for each cell type).

DC. Although both subsets could take up, process, and present recombinant protein to CD4^{+} T cells and CD8^{+} T cells, CD141^{+} DCs were more efficient as individual cells in cross-presenting recombinant protein to CD8^{+} T cells after activation with poly I:C. Most importantly, unlike CD1c^{+} DC, the CD141^{+} DC subset was able to cross-present viral Ag from HCMV-infected necrotic fibroblasts. These data establish CD141^{+} DC and CD1c^{+} DC as functionally distinct subsets and highlight the emerging complexity and specialized roles of human DC subtypes. Although rare in human blood, our study and others showed that CD141^{+} DCs are also found in lymph nodes, tonsil, bone marrow, and spleen where they localize to the T cell areas (Galibert et al., 2005; Velásquez-Lopera et al., 2008). Moreover, they are present in proportions that are similar to or higher than those of CD1c^{+} DCs in tonsil and spleen (Velásquez-Lopera et al., 2008; unpublished data). Collectively, these data suggest that CD141^{+} DCs are likely to be of profound importance in the induction of Th1 responses and CTL responses by cross-presentation.

Our data reveal remarkable functional similarities between human CD141^{+} DC and mouse CD8α^{+} DC, which, combined with similarities in their transcriptomes (Robbins et al., 2008) and shared expression of CLEC9A (Caminschi et al., 2008; Huysamen et al., 2008; Sancho et al., 2008) and Necl2 (Galibert et al., 2005), supports the hypothesis that these subsets have related functions. Both are extremely rare in blood but are present in the T cell areas of lymphoid tissues where their functions are mediated (Shortman and Liu, 2002; O'Keeffe et al., 2003; Galibert et al., 2005). Like human CD141^{+} DCs, mouse CD8α^{+} DCs express high levels of TLR3 (Edwards et al., 2003) and produce IFN-β in response to poly I:C (Scheu et al., 2008). Mouse CD8α[+] DCs are renowned for their ability to produce IL-12p70 (Reis e Sousa et al., 1997; Maldonado-López et al., 1999; Hochrein et al., 2001) and induce the Th1 cytokines IL-2 and IFN-γ (Maldonado-López et al., 1999; Pulendran et al., 1999; Skokos and Nussenzweig, 2007; Soares et al., 2007), which concurs with our human CD141^{+} DC data. Extending this comparison, the lack of IL-12p70 release by CD141^{+} DC in response to poly I:C and CD40L suggests this subset can induce Th1 responses independently of IL-12p70, as can mouse CD8α^{+} DCs (Soares et al., 2007). Most importantly, like human CD141^{+} DCs, mouse CD8α^{+} DCs have specialized cross-presenting capacity, particularly after taking up dead/dying cells or after poly I:C activation (den Haan et al., 2000; Iyoda et al., 2002; Schulz et al., 2005; Schnorrer et al., 2006). Their mutual expression of high levels of MHC class I Ag-processing molecules (Dudziak et al., 2007) and TLR3 and CLEC9A, which both act as sensors of necrotic cells and regulators of cross-priming in mice (Schulz et al., 2005; Cavassani et al., 2008; Sancho et al., 2009), are likely to facilitate this process. The crucial role of mouse CD8α[+] DC in the induction of protective CTL responses in tumor and viral models has been confirmed in vivo (Dudziak et al., 2007; Hildner et al., 2008; López-Bravo and Ardavín, 2008; Naik, 2008). CD8α[+] DCs also cross-present parasite Ag and mediate CTL responses against blood stage *Plasmodium* (Lundie et al., 2008). Based on their functional similarities to mouse CD8α^{+} DCs in vitro, these data lend further support to the hypothesis that CD141^{+} DCs will be the major human DC subset involved in the induction of CTL responses against tumors and many pathogens.

Despite their similarities, there are also notable differences between human CD141^{+} DCs and mouse CD8α^{+} DCs. Unlike human CD141^{+} DCs, mouse CD8α^{+} DCs express TLR4 and 9 and, thus, should respond differently to their ligands (Edwards et al., 2003). The transcription factors *IRF8* and *Batf3*, which are known to be essential for mouse CD8α^{+} DC differentiation (Schiavoni et al., 2002; Aliberti et al., 2003; Hildner et al., 2008), were not selectively expressed by CD141^{+} DC. However, once differentiated, mouse CD8α^{+} and CD8α^{-} DCs also express similar levels of Batf3 (Hildner et al., 2008), so our data does not exclude a role for these transcription factors in human CD141^{+} DC early development. The ability to cross-present soluble protein was not unique to CD141^{+} DCs in humans, even though they were more efficient than CD1c^{+} DCs on a per cell basis after activation. This is not dissimilar to mouse DC because although CD8α^{+} DCs are clearly the major subset involved in cross-presentation, other mouse DC subsets, such as Langerhans cells and dermal CD103^{+} DC, also have cross-presenting capacity (Stoitzner et al., 2006; Bedoui et al., 2009b). In most donors, CD141^{+} DC required poly I:C activation in order to up-regulate MHC class I processing molecules and induce cross-presentation of protein Ag, whereas these features are characteristic of CD8α[+] DC, even in the absence of activation (Pooley et al., 2001; Schnorrer et al., 2006). Further studies will be necessary to establish whether these represent interspecies differences in DC function or could be explained by their tissue locality (human DCs are isolated from blood, whereas mouse DCs are generally isolated from spleen). Transcriptome differences between the human DC subsets isolated from blood and tonsil reinforces the latter possibility (Lindstedt et al., 2005). Blood CD141^{+} DCs may be a precursor of their lymphoid tissue counterparts, similar to the recently described mouse splenic CD8α^{+} DC precursor population defined as CD8α^{-}CD24^{+} DCs, which are phenotypically similar and cross-present but with lower efficiency than CD8α^{+} DCs (Bedoui et al., 2009a). Interestingly, mouse CD8α^{-}CD24^{+} DCs are also very rare (∼2% of DC in mouse spleen) but are more effective than CD8α^{+} DCs at inducing T cell responses and promoting viral clearance.

The human CD1c^{+} DC subset is hypothesized to be similar to the mouse CD8α^{-} DC subset, and our data reinforces this further alignment of the human and mouse DC subsets (Robbins et al., 2008). Like human CD1c^{+} DCs, mouse CD8α^{-} DCs are poor producers of IFN-β and IL-12p70 and are not major inducers of Th1 responses (Maldonado-López et al., 1999; Pulendran et al., 1999). Unlike CD1c^{+} DCs, mouse CD8α^{-} DCs preferentially induce Th2 responses (Maldonado-López et al., 1999; Pulendran et al., 1999). Mouse CD8α^{-} DCs are specialized at presenting Ag to

JEM

CD4^{+} T cells after chimeric Ab-mediated delivery of Ag (Dudziak et al., 2007). However, this may be restricted to certain types of Ag delivery strategies, as mouse CD8α^{+} DCs are similarly efficient at presenting soluble protein, *Escherichia coli*–derived Ag, dead cell Ag, and viral particles to CD4^{+} T cells (Schnorrer et al., 2006; Keller et al., 2010). Our study showed that CD1c^{+} DC and CD141^{+} DC had a similar capacity to present protein Ag to CD4^{+} T cells and, in this regard, the human subsets are similar to their mouse counterparts. Neither CD1c^{+} DCs nor CD8α^{−} DCs (Pooley et al., 2001; Schnorrer et al., 2006; Dudziak et al., 2007) are efficient at cross-presenting necrotic cell Ag to CD8^{+} T cells, but we found that CD1c^{+} DCs cross-present soluble protein to a limited extent in the presence or absence of exogenous stimuli, which is consistent with another study (Schnurr et al., 2005). Human DC subsets may be specialized at cross–presenting particular types of Ag for different functional outcomes, such as priming or tolerance (Burgdorf and Kurts, 2008), and this will be an important area for future investigation.

The limited capacity of CD1c^{+} DC to produce IL-12p70 and CXCL10 and augment Th1 responses and cross-presentation after poly I:C activation appears to be an intrinsic feature of this subset rather than a specific outcome of ineffi-cient TLR3 stimulation. Our data and that of others suggest that CD1c^{+} DCs are similarly ineffective in this regard after activation with other stimuli, including TLR4, 7, and 8 ago-nists, CD40L, and whole *E. coli* (Luft et al., 2002; Jefford et al., 2003; Piccioli et al., 2007). Selective expression of SIRP-α (signal regulatory protein α) by mouse CD8α^{−} DC and human CD1c^{+} DC (Lindstedt et al., 2005; Lahoud et al., 2006) may account for their lack of IFN-β production after poly I:C activation (Dong et al., 2008). However, CD1c^{+} DCs are clearly capable of responding in other ways to poly I:C and, indeed, produced similar levels of IL-6, IL-8, and TNF and higher levels of IL-1β than CD141^{+} DCs after poly I:C stimulation. Poly I:C and dsRNA have recently been shown to signal through the RNA helicase RIG-1 in addition to TLR3 (Nakhaei et al., 2009), and signaling via this path-way results in inflammasome activation and IL-1β production (Poeck et al., 2010). RIG-1 is selectively expressed by mouse CD8α^{−} DCs (Luber et al., 2010), and it is likely that CD1c^{+} DCs also respond to poly I:C via this alternate pathway.

The identification of the human DC subset with similar functions to mouse CD8α^{+} DC will facilitate translation of the wealth of knowledge on mouse DC into clinical practice. This has clear implications for the design of new therapies to treat cancers and infectious diseases. Our data suggests that CD141^{+} DC will be the main human DC subset involved in stimulating CTL responses and the most appropriate one to target for therapeutic cancer, viral, and other pathogen (e.g., malaria) vaccines. The latter is supported by the detection of increased frequencies of circulating CD141^{+} DC, but not CD1c^{+} DC, in severe malaria (Urban et al., 2006). The cur-rent clinical methods for manipulating human DC ex vivo are unlikely to be practical for CD141^{+} DC isolation. How-ever, targeting Ag directly in vivo with DC-specific Ab is a highly attractive concept to enhance specificity and efficacy and improve the logistics, cost, and availability of therapeutic vaccines (Steinman, 2008). Monoclonal Abs against CLEC9A and CD205 have demonstrated efficacy in inducing potent antitumor and antiviral immunity by delivering Ag to mouse CD8α^{+} DC in vivo (Bonifaz et al., 2004; Sancho et al., 2008). CLEC9A and CD205 are also expressed by human CD141^{+} DC, and our data gives proposed clinical vaccina-tion studies using these targets new impetus and may extend to other therapeutic strategies that regulate DC in transplan-tation and autoimmune disease.

MATERIALS AND METHODS

Flow cytometry phenotyping. Healthy donor peripheral blood, leuka-pheresis products, bone marrow, and tonsil were obtained with informed consent after approval by the Mater Health Services Human Research Ethics Committee. CLEC9A Abs were gifts from M. Lahoud and K. Shortman (Walter and Eliza Hall Institute, Melbourne, Victoria, Australia) and G. Brown (University of Cape Town, Observatory, South Africa). Cells were labeled with combinations of PE–, FITC–, and allophycocyanin (APC)–Cy7–conjugated mouse anti–human lineage Ab (CD3, CD19, CD20, CD34, and CD56), CD11c, CD40, CD80, CD83, CD86, HLA-ABC, and HLA-DR Ab, or isotype controls (all obtained from BD). Cell acquisition was performed on a flow cytometer (LSR II; BD) and analyzed using FlowJo (version 7.2.2; Tree Star, Inc.). For TLR3 staining, DCs were fixed and permeabilized us-ing Fixation/Permeabilization buffers (eBioscience), according to the manu-facturer's instructions, before intracellular labeling with TLR3 or IgG isotype control Ab (eBioscience).

Immunohistochemistry staining of human lymph nodes. Lymph nodes that were as close as possible to normal lymph nodes were obtained from living donors undergoing surgery and donors postmortem, with no ab-normality detected after a histopathology examination (provided by T. John, J. Browning, D. MacGregor, and J. Cebon, Ludwig Institute of Cancer Re-search, Melbourne, Victoria, Australia). Lymph nodes were obtained from the axillary and inguinal fields. Patients or the next of kin gave written in-formed consent, under protocols approved by the Austin Health Human Research Ethics Committee, Heidelberg, Melbourne.

Lymph nodes were embedded in Tissue Tek OCT compound (Sakura), snap frozen in liquid nitrogen, and sectioned using a cryostat. Sections 5-μm thick were fixed with ice-cold acetone and blocked with serum-free protein block (Dako). Fixed sections were probed with mouse monoclonal Ab against CLEC9A and CD209 (BD) and a rabbit polyclonal Ab detecting CD3 (Invitrogen). The primary Abs were detected with the correspond-ing isotype-specific goat anti–mouse or goat anti–rabbit secondary Ab conjugated to a fluorochrome (Alexa Fluor 350, 488, or 555; Invitrogen). The specificity of each secondary Ab was confirmed using an isotype- or species-mismatched primary Ab. DAPI was included at 0.0005% wt/vol with the secondary Ab. The slides were mounted using Prolong Gold (Invi-trogen). Sections were visualized with a fluorescent microscope (DMRE; Leica) equipped with UV, 470–490-μm, and 515–560-μm epi fluorescent filters (Leica). Images were acquired at room temperature using 5×/0.15 NA, 10×/0.30 NA, 20×/0.50 NA, and 40×/0.7 NA Leica objectives, a digital camera (DC500; Leica), and analySIS FIVE software (Olympus). Images were processed using Portia image manipulation software (CytoCode Software).

DC isolations. PBMCs were isolated from leukapheresis products using Ficoll-Paque Plus density gradient centrifugation (GE Healthcare). CD141^{+} DCs were isolated by an initial immunomagnetic depletion of lineage-positive mononuclear cells followed by flow cytometry sorting. Briefly, PBMCs were labeled with a primary mouse anti–human monoclonal Ab cocktail containing CD3 (American Type Culture Collection), CD14, CD16, CD19, CD20, CD56 (all from Beckman Coulter), CD34, and CD235a (BD) in

Downloaded from http://rupress.org/jem/article-pdf/207/6/1247/1739113/jem_20092140.pdf by guest on 09 February 2026

1256   The function of human CD141^{+} dendritic cells | Jongbloed et al.

cold PBS supplemented with 0.5% BSA (Invitrogen) and 2 mM EDTA (Merck). After washing, cells were incubated with goat anti–mouse IgG microbeads (Miltenyi Biotec), and labeled cells were magnetically depleted using an autoMACS (Miltenyi Biotec). CD141$^+$ DCs were further purified by labeling the lineage-negative enriched fraction with CD141-APC, CD304-PE (Miltenyi Biotec), CD15- (BD), CD1b/c- (Gen-Probe), and sheep anti–mouse- (Millipore) FITC and were sorted as CD141-APC$^+$FITC$^-$PE$^-$ events using a FACSAria cell sorter (BD). CD1c$^+$ DCs were isolated from the same PBMC by positive immunoselection using the BDCA-1$^+$ DC isolation kit (Miltenyi Biotec) and were further purified by staining and flow cytometry sorting of CD1b/c-FITC$^+$, lin-PE$^-$ (BD), and CD141-APC$^-$ events. These procedures routinely yielded CD141$^+$ and CD1c$^+$ DC preparations of >99% purity. CD16$^+$ DCs were isolated with a similar procedure to the CD141$^+$ DC isolations using an initial lineage depletion step (excluding CD16 from the Ab cocktail), followed by flow sorting of lineage-FITC$^-$CD16-PE$^+$ events. MoDC were differentiated from monocytes that were isolated by CD14$^+$ immunomagnetic selection (Miltenyi Biotec) and cultured for 5–6 d in complete AB medium supplemented with 800 U/ml GM-CSF (Invitrogen) and 1,000 U/ml IL-4 (Invitrogen) as previously described (Radford et al., 2006).

Cells were maintained in complete AB medium consisting of RPMI 1640, supplemented with 10% heat-inactivated human AB serum, 100 U/ml penicillin, 100 µg/ml streptomycin, 2 mM L-glutamine, 1 mM sodium pyruvate, 0.1 mM nonessential amino acids, 10 mM Hepes buffer solution (all obtained from Invitrogen), and 50 µM 2-mercaptoethanol (Sigma-Aldrich) and were cultured in a 37°C, 5% CO$_2$/air atmosphere incubator. Where indicated, DCs were cultured in complete AB medium for 24 h alone or in the presence of 10 µg/ml LPS–free poly I:C (InvivoGen).

Quantitative RT-PCR. Total RNA was isolated from cells with the RNeasy Micro kit (QIAGEN). RNA was treated with DNase I to remove contaminating genomic DNA and subjected to cDNA synthesis using a (dT)17 primer (Roche) and Superscript III Reverse transcription (Invitrogen). PCR reactions for TLR1–8 and TLR10 were performed on a Thermo Cycler (MJ Research) using Taq DNA polymerase (QIAGEN) and primers and conditions previously described (Kadowaki et al., 2001). PCR for TLR9 and UCE (Table S1, primer sequences) were performed under similar conditions, except that the annealing temperature for TLR9 was 65°C. TLR3 real-time PCR reactions were performed with TaqMan probes (Biosearch Technologies) and Platinum Quantitative PCR SuperMix-UDG (Invitrogen). UCE was used for normalization of cDNA input, and real-time PCR reactions were performed using a Rotor-Gene 3000 thermal cycler (QIAGEN). The thermal cycling conditions were initial denaturation of UDG (uracil DNA glycosylase) at 50°C for 2 min, followed by 45–50 cycles at 95°C for 15 s and at 60°C for 30 s.

Real-time PCR reactions for *IRF8*, *TYROBP*, *BATF3*, *IFI30*, *HLA-DMA*, *CTSH*, *TAP1*, *TAP2*, *SEC61A*, and *UBC* were performed with SuperArray RT^2 qPCR Primers (QIAGEN; Table S1) and RT^2 SYBR Green qPCR master mix (QIAGEN). UBC was used for normalization of cDNA input, and real-time PCR reactions were performed using a Rotor-Gene 3000 thermal cycler according to the manufacturer's instructions: initial denaturation at 95°C for 10 min, followed by 45–50 cycles at 95°C for 15 s and at 60°C for 60 s. All real-time PCR data analysis was performed using Rotor-Gene 6.0 software (QIAGEN) and the $\Delta\Delta C_t$ method.

Cytokine secretion assays. Culture supernatants were harvested and levels of IL-10, TNF, IL-1β, IL-6, IL-8, CXCL10, IL-2, and IFN-γ were determined using Flow Cytometric Bead Arrays (BD) according to the manufacturer's instructions. IFN-β (PBL Biomedical Laboratories) secretion was detected by ELISA according to the manufacturer's instructions. IL-12p70 secretion was detected by ELISA (Thermo Fisher Scientific) after incubation of DC with an activation cocktail (Mailliard et al., 2004) consisting of 25 µg/ml poly (I:C), 1,000 U/ml IFN-γ (R&D Systems), 50 ng/ml TNF (R&D Systems), 3,000 U/ml IFN-α (R&D Systems), and 25 ng/ml IL-1β (R&D Systems).

Allogeneic MLR. Allogeneic CD4$^+$ T cells were isolated from PBMC by negative immunomagnetic selection after labeling with mouse monoclonal Ab to human CD8, CD14, CD16, CD19, CD34, CD56, HLA-DR, and CD235a, followed by goat anti–mouse IgG microbeads (Miltenyi Biotec) and separation using an autoMACS device. Donor-matched CD141$^+$ DC and CD1c$^+$ DC were cultured for 18 h with or without poly I:C and then washed and used to stimulate allogeneic CD4$^+$ T cells at a ratio of 1:10. Wells containing CD4$^+$ T cells, or poly I:C–stimulated or unstimulated DC alone, were included as controls. Cells were cultured for 6 d and T cell proliferation was measured by ^{3}[H]-thymidine incorporation during the last 16 h of culture. Cytokines were measured in the culture supernatants after 6 d using Flow Cytometric Bead Arrays (BD).

Uptake, processing, and presentation of recombinant pp65 protein. To examine uptake of soluble protein, DCs were incubated at 4 or 37°C in the absence or presence of poly I:C with 1 mg/ml Lucifer yellow CH Dipotassium Salt (Sigma-Aldrich) for 1 h, washed four times in ice-cold PBS/0.5% FCS, and then analyzed by flow cytometry. For processing and presentation assays, DCs from HCMV sero-positive donors were loaded with 38.5 µg/ml of recombinant HCMVpp65 protein (Miltenyi Biotec) for 2 h in the absence or presence of poly I:C. Equivalent numbers of CD141$^+$ DC and CD1c$^+$ DC (50,000/well) were washed and incubated for 16 h with autologous PBMC at a 1:20 ratio. Ag-specific T cell stimulation was then assayed by intracellular IFN-γ staining. Briefly, cultures were incubated in GolgiPlug (BD) for 4 h and then stained with mouse anti–human CD3-APC, CD4-APC-Cy-7, and CD8-FITC, followed by fixing and permeabilization using a kit (Invitrogen) and intracellular staining with anti–IFN-γ-PE or IgG-PE isotype control (BD) and analyzed by flow cytometry. The percentage of responding CD4$^+$ or CD8$^+$ T cells was calculated as the percentage of CD3$^+$CD8$^-$CD4$^+$IFN-γ$^+$ or CD3$^+$CD8$^+$CD4$^-$IFN-γ$^+$ events after subtraction of the respective IgG-PE isotype control.

To examine CD8$^+$ T cell responses specific for the HLA-A*0201-restricted HCMV pp65$_{495-503}$ epitope, DCs from HLA-A*0201$^+$ donors were cultured alone or with 10 µg/ml HCMVpp65 protein, pp65$_{495-503}$ peptide (NLVPMVATV; ProImmune), or irrelevant control peptide for 2 h in the absence or presence of poly I:C. For some experiments, DCs were cultured with 10 µm lactacystin (Sigma-Aldrich) for 45 min before adding Ag. These conditions have been previously shown to be nontoxic to human cells (Schnurr et al., 2005). DCs were then washed and equivalent numbers of CD141$^+$ DC and CD1c$^+$ DC (25,000/well) exposed to a pp65$_{495-503}$–specific CD8$^+$ T cell line for 16 h at a 1:2 ratio. Ag-specific T cell stimulation was then assayed by intracellular IFN-γ staining as described in the previous paragraph.

Uptake and processing of HCMV-infected necrotic fibroblasts. The HLA-A*0201$^-$ human neonatal foreskin fibroblast cell line NFF59 was infected with the HCMV AD169 strain (Arrode et al., 2000; both gifts from R. Khanna, Queensland Institute of Medical Research, Queensland, Australia) at a preoptimized multiplicity of infection of 3 for 24 h, which resulted in 65% infection (Fig. S4). Secondary necrosis was induced by UV irradiation of the fibroblasts at 302 nm for 60 min, followed by culture for a further 24 h, by which time >95% of fibroblasts stained positive for Annexin-V and propidium iodide (Fig. S4). Uninfected and HCMV-infected necrotic fibroblasts were co-cultured with DC at a 1:1 ratio for 12 h, and Ag uptake and cross-presentation were examined as described in the next two paragraphs.

For uptake experiments, fibroblasts were initially labeled with 10 µM PKH-26 (Sigma-Aldrich), according to the manufacturer's instructions, before HCMV infection and UV irradiation. DCs were incubated at 4 or 37°C in the absence or presence of HCMV-infected necrotic fibroblasts for 12 h, stained with mouse anti–human CD11c-APC and HLA-DR-APC-Cy7 for analysis by flow cytometry, or stained and analyzed by confocal microscopy. For confocal microscopy, cells were labeled with HLA-DR-FITC, before being fixed with 4% paraformaldehyde and allowed to dry on microscope slides, and then mounted with prolong gold + DAPI (Invitrogen). Cells were viewed on a laser-scanning microscope (510 META; Carl Zeiss, Inc.) through a

63×/1.4 oil DIC Plan-Apochromat or 100×/1.3 oil EC Plan-Neofluar lens (Carl Zeiss, Inc.) at 21°C. Cell images were acquired using LSM 510 software (version 4.0).

For Ag-processing experiments, equivalent numbers of CD141+ DC and CD1c+ DC (13,000–20,000/well) were washed and used to stimulate a pp65$_{495-503}$-specific CD8+ T cell line at a 1:10 ratio. Cross-presentation was measured as IFN-γ production by the T cell line by ELISA (eBioscience) after 24 h.

Statistics. Significance was evaluated using a two-tailed Mann Whitney test for unpaired data or a two-tailed Wilcoxin signed rank test for paired data.

Online supplemental material. Fig. S1 shows expression of transcription factors *Batf3*, *IRF8*, and *TYROBP* by CD141+ DC and CD1c+ DC. Fig. S2 shows the TLR expression profile of CD1c+ DC. Fig. S3 compares the effect of LPS and poly I:C activation on CD1c+ DC cytokine secretion and Th1- and cross-presenting capacity. Fig. S4 shows the HCMV AD169 infection by fibroblasts, but not DC, and the induction of necrosis in AD169-infected fibroblasts. Table S1 provides a list of PCR primers. Online supplemental material is available at http://www.jem.org/cgi/content/full/jem.20092140/DC1.

REFERENCES

Alexander, J., and E. McFarlane. 2008. Can type-1 responses against intracellular pathogens be T helper 2 cytokine dependent? *Microbes Infect.* 10:953–959. doi:10.1016/j.micinf.2008.07.038

Aliberti, J., O. Schulz, D.J. Pennington, H. Tsujimura, C. Reis e Sousa, K. Ozato, and A. Sher. 2003. Essential role for ICSBP in the in vivo development of murine CD8alpha + dendritic cells. *Blood.* 101:305–310. doi:10.1182/blood-2002-04-1088

Angel, C.E., C.J. Chen, O.C. Horlacher, S. Winkler, T. John, J. Browning, D. MacGregor, J. Cebon, and P.R. Dunbar. 2009. Distinctive localization of antigen-presenting cells in human lymph nodes. *Blood.* 113:1257–1267. doi:10.1182/blood-2008-06-165266

Arrode, G., C. Boccaccio, J. Lulé, S. Allart, N. Moinard, J.P. Abastado, A. Alam, and C. Davrinche. 2000. Incoming human cytomegalovirus pp65 (UL83) contained in apoptotic infected fibroblasts is cross-presented to CD8(+) T cells by dendritic cells. *J. Virol.* 74:10018–10024. doi:10.1128/JVI.74.21.10018-10024.2000

Bedoui, S., S. Prato, J. Mintern, T. Gebhardt, Y. Zhan, A.M. Lew, W.R. Heath, J.A. Villadangos, and E. Segura. 2009a. Characterization of an immediate splenic precursor of CD8+ dendritic cells capable of inducing antiviral T cell responses. *J. Immunol.* 182:4200–4207. doi:10.4049/jimmunol.0802286

Bedoui, S., P.G. Whitney, J. Waithman, L. Eidsmo, L. Wakim, I. Caminschi, R.S. Allan, M. Wojtasiak, K. Shortman, F.R. Carbone, et al. 2009b. Cross-presentation of viral and self antigens by skin-derived CD103+ dendritic cells. *Nat. Immunol.* 10:488–495. doi:10.1038/ni.1724

Bonifaz, L.C., D.P. Bonnyay, A. Charalambous, D.I. Darguste, S. Fujii, H. Soares, M.K. Brimnes, B. Moltedo, T.M. Moran, and R.M. Steinman. 2004. In vivo targeting of antigens to maturing dendritic cells via the DEC-205 receptor improves T cell vaccination. *J. Exp. Med.* 199:815–824. doi:10.1084/jem.20032220

Burgdorf, S., and C. Kurts. 2008. Endocytosis mechanisms and the cell biology of antigen presentation. *Curr. Opin. Immunol.* 20:89–95. doi:10.1016/j.coi.2007.12.002

Caminschi, I., A.I. Proietto, F. Ahmet, S. Kitsoulis, J. Shin Teh, J.C. Lo, A. Rizzitelli, L. Wu, D. Vremec, S.L. van Dommelen, et al. 2008. The dendritic cell subtype-restricted C-type lectin Clec9A is a target for vaccine enhancement. *Blood.* 112:3264–3273. doi:10.1182/blood-2008-05-155176

Cavassani, K.A., M. Ishii, H. Wen, M.A. Schaller, P.M. Lincoln, N.W. Lukacs, C.M. Hogaboam, and S.L. Kunkel. 2008. TLR3 is an endogenous sensor of tissue necrosis during acute inflammatory events. *J. Exp. Med.* 205:2609–2621. doi:10.1084/jem.20081370

den Haan, J.M., S.M. Lehar, and M.J. Bevan. 2000. CD8+ but not CD8− dendritic cells cross-prime cytotoxic T cells in vivo. *J. Exp. Med.* 192:1685–1696. doi:10.1084/jem.192.12.1685

Dong, L.W., X.N. Kong, H.X. Yan, L.X. Yu, L. Chen, W. Yang, Q. Liu, D.D. Huang, M.C. Wu, and H.Y. Wang. 2008. Signal regulatory protein alpha negatively regulates both TLR3 and cytoplasmic pathways in type I interferon induction. *Mol. Immunol.* 45:3025–3035. doi:10.1016/j.molimm.2008.03.012

Dudziak, D., A.O. Kamphorst, G.F. Heidkamp, V.R. Buchholz, C. Trumpfheller, S. Yamazaki, C. Cheong, K. Liu, H.W. Lee, C.G. Park, et al. 2007. Differential antigen processing by dendritic cell subsets in vivo. *Science.* 315:107–111. doi:10.1126/science.1136080

Dzionek, A., A. Fuchs, P. Schmidt, S. Cremer, M. Zysk, S. Miltenyi, D.W. Buck, and J. Schmitz. 2000. BDCA-2, BDCA-3, and BDCA-4: three markers for distinct subsets of dendritic cells in human peripheral blood. *J. Immunol.* 165:6037–6046.

Edwards, A.D., S.S. Diebold, E.M. Slack, H. Tomizawa, H. Hemmi, T. Kaisho, S. Akira, and C. Reis e Sousa. 2003. Toll-like receptor expression in murine DC subsets: lack of TLR7 expression by CD8 alpha+ DC correlates with unresponsiveness to imidazoquinolines. *Eur. J. Immunol.* 33:827–833. doi:10.1002/eji.200323797

Galibert, L., G.S. Diemer, Z. Liu, R.S. Johnson, J.L. Smith, T. Walzer, M.R. Comeau, C.T. Rauch, M.F. Wolfson, R.A. Sorensen, et al. 2005. Nectin-like protein 2 defines a subset of T-cell zone dendritic cells and is a ligand for class-I–restricted T-cell-associated molecule. *J. Biol. Chem.* 280:21955–21964. doi:10.1074/jbc.M502095200

Hart, D.N. 1997. Dendritic cells: unique leukocyte populations which control the primary immune response. *Blood.* 90:3245–3287.

Hildner, K., B.T. Edelson, W.E. Purtha, M. Diamond, H. Matsushita, M. Kohyama, B. Calderon, B.U. Schraml, E.R. Unanue, M.S. Diamond, et al. 2008. Batf3 deficiency reveals a critical role for CD8alpha+ dendritic cells in cytotoxic T cell immunity. *Science.* 322:1097–1100. doi:10.1126/science.1164206

Hochrein, H., K. Shortman, D. Vremec, B. Scott, P. Hertzog, and M. O'Keeffe. 2001. Differential production of IL-12, IFN-alpha, and IFN-gamma by mouse dendritic cell subsets. *J. Immunol.* 166:5448–5455.

Huysamen, C., J.A. Willment, K.M. Dennehy, and G.D. Brown. 2008. CLEC9A is a novel activation C-type lectin-like receptor expressed on BDCA3+ dendritic cells and a subset of monocytes. *J. Biol. Chem.* 283:16693–16701. doi:10.1074/jbc.M709923200

Iyoda, T., S. Shimoyama, K. Liu, Y. Omatsu, Y. Akiyama, Y. Maeda, K. Takahara, R.M. Steinman, and K. Inaba. 2002. The CD8+ dendritic cell subset selectively endocytoses dying cells in culture and in vivo. *J. Exp. Med.* 195:1289–1302. doi:10.1084/jem.20020161

Jefford, M., M. Schnurr, T. Toy, K.A. Masterman, A. Shin, T. Beecroft, T.Y. Tai, K. Shortman, M. Shackleton, I.D. Davis, et al. 2003. Functional comparison of DCs generated in vivo with Flt3 ligand or in vitro from blood monocytes: differential regulation of function by specific classes of physiologic stimuli. *Blood.* 102:1753–1763. doi:10.1182/blood-2002-12-3854

Kadowaki, N., S. Ho, S. Antonenko, R.W. Malefyt, R.A. Kastelein, F. Bazan, and Y.J. Liu. 2001. Subsets of human dendritic cell precursors express different toll-like receptors and respond to different microbial antigens. *J. Exp. Med.* 194:863–869. doi:10.1084/jem.194.6.863

Karikó, K., H. Ni, J. Capodici, M. Lamphier, and D. Weissman. 2004. mRNA is an endogenous ligand for Toll-like receptor 3. *J. Biol. Chem.* 279:12542–12550. doi:10.1074/jbc.M310175200

Keller, S.A., M. Bauer, V. Manolova, S. Muntwiler, P. Saudan, and M.F. Bachmann. 2010. Cutting edge: limited specialization of dendritic cell subsets for MHC class II-associated presentation of viral particles. *J. Immunol.* 184:26–29. doi:10.4049/jimmunol.0901540

Kyte, J.A., S. Trachsel, B. Risberg, P. thor Straten, K. Lislerud, and G. Gaudernack. 2009. Unconventional cytokine profiles and development of T cell memory in long-term survivors after cancer vaccination. *Cancer Immunol. Immunother.* 58:1609–1626. doi:10.1007/s00262-009-0670-2

Lahoud, M.H., A.I. Proietto, K.H. Gartlan, S. Kitsoulis, J. Curtis, J. Wettenhall, M. Sofi, C. Daunt, M. O'keeffe, I. Caminschi, et al. 2006. Signal regulatory protein molecules are differentially expressed by CD8- dendritic cells. *J. Immunol.* 177:372–382.

Le Bon, A., and D.F. Tough. 2008. Type I interferon as a stimulus for cross-priming. *Cytokine Growth Factor Rev.* 19:33–40. doi:10.1016/j.cytogfr.2007.10.007

Lindell, D.M., T.E. Lane, and N.W. Lukacs. 2008. CXCL10/CXCR3-mediated responses promote immunity to respiratory syncytial virus infection by augmenting dendritic cell and CD8(+) T cell efficacy. *Eur. J. Immunol.* 38:2168–2179. doi:10.1002/eji.200838155

Lindstedt, M., K. Lundberg, and C.A. Borrebaeck. 2005. Gene family clustering identifies functionally associated subsets of human in vivo blood and tonsillar dendritic cells. *J. Immunol.* 175:4839–4846.

López-Bravo, M., and C. Ardavín. 2008. In vivo induction of immune responses to pathogens by conventional dendritic cells. *Immunity.* 29:343–351. doi:10.1016/j.immuni.2008.08.008

Luber, C.A., J. Cox, H. Lauterbach, B. Fancke, M. Selbach, J. Tschopp, S. Akira, M. Wiegand, H. Hochrein, M. O'Keeffe, and M. Mann. 2010. Quantitative proteomics reveals subset-specific viral recognition in dendritic cells. *Immunity.* 32:279–289. doi:10.1016/j.immuni.2010.01.013

Luft, T., M. Jefford, P. Luetjens, T. Toy, H. Hochrein, K.A. Masterman, C. Maliszewski, K. Shortman, J. Cebon, and E. Maraskovsky. 2002. Functionally distinct dendritic cell (DC) populations induced by physiologic stimuli: prostaglandin E(2) regulates the migratory capacity of specific DC subsets. *Blood.* 100:1362–1372. doi:10.1182/blood-2001-12-0360

Lundie, R.J., T.F. de Koning-Ward, G.M. Davey, C.Q. Nie, D.S. Hansen, L.S. Lau, J.D. Mintern, G.T. Belz, L. Schofield, F.R. Carbone, et al. 2008. Blood-stage Plasmodium infection induces CD8+ T lymphocytes to parasite-expressed antigens, largely regulated by CD8alpha+ dendritic cells. *Proc. Natl. Acad. Sci. USA.* 105:14509–14514. doi:10.1073/pnas.0806727105

MacDonald, K.P., D.J. Munster, G.J. Clark, A. Dzionek, J. Schmitz, and D.N. Hart. 2002. Characterization of human blood dendritic cell subsets. *Blood.* 100:4512–4520. doi:10.1182/blood-2001-11-0097

Mailliard, R.B., A. Wankowicz-Kalinska, Q. Cai, A. Wesa, C.M. Hilkens, M.L. Kapsenberg, J.M. Kirkwood, W.J. Storkus, and P. Kalinski. 2004. alpha-type-1 polarized dendritic cells: a novel immunization tool with optimized CTL-inducing activity. *Cancer Res.* 64:5934–5937. doi:10.1158/0008-5472.CAN-04-1261

Maldonado-López, R., T. De Smedt, P. Michel, J. Godfroid, B. Pajak, C. Heirman, K. Thielemans, O. Leo, J. Urbain, and M. Moser. 1999. CD8α^+ and CD8α^- subclasses of dendritic cells direct the development of distinct T helper cells in vivo. *J. Exp. Med.* 189:587–592. doi:10.1084/jem.189.3.587

Matsumoto, M., K. Funami, M. Tanabe, H. Oshiumi, M. Shingai, Y. Seto, A. Yamamoto, and T. Seya. 2003. Subcellular localization of Toll-like receptor 3 in human dendritic cells. *J. Immunol.* 171:3154–3162.

Naik, S.H. 2008. Demystifying the development of dendritic cell subtypes, a little. *Immunol. Cell Biol.* 86:439–452. doi:10.1038/icb.2008.28

Nakhaei, P., P. Genin, A. Civas, and J. Hiscott. 2009. RIG-I-like receptors: sensing and responding to RNA virus infection. *Semin. Immunol.* 21:215–222. doi:10.1016/j.smim.2009.05.001

O'Keeffe, M., H. Hochrein, D. Vremec, B. Scott, P. Hertzog, L. Tatarczuch, and K. Shortman. 2003. Dendritic cell precursor populations of mouse blood: identification of the murine homologues of human blood plasmacytoid pre-DC2 and CD11c+ DC1 precursors. *Blood.* 101:1453–1459. doi:10.1182/blood-2002-03-0974

Orabona, C., P. Puccetti, C. Vacca, S. Bicciato, A. Luchini, F. Fallarino, R. Bianchi, E. Velardi, K. Perruccio, A. Velardi, et al. 2006. Toward the identification of a tolerogenic signature in IDO-competent dendritic cells. *Blood.* 107:2846–2854. doi:10.1182/blood-2005-10-4077

Piccioli, D., S. Tavarini, E. Borgogni, V. Steri, S. Nuti, C. Sammicheli, M. Bardelli, D. Montagna, F. Locatelli, and A. Wack. 2007. Functional specialization of human circulating CD16 and CD1c myeloid dendritic-cell subsets. *Blood.* 109:5371–5379. doi:10.1182/blood-2006-08-038422

Poeck, H., M. Bscheider, O. Gross, K. Finger, S. Roth, M. Rebsamen, N. Hannesschläger, M. Schlee, S. Rothenfusser, W. Barchet, et al. 2010. Recognition of RNA virus by RIG-I results in activation of CARD9 and inflammasome signaling for interleukin 1 beta production. *Nat. Immunol.* 11:63–69. doi:10.1038/ni.1824

Pooley, J.L., W.R. Heath, and K. Shortman. 2001. Cutting edge: intravenous soluble antigen is presented to CD4 T cells by CD8- dendritic cells, but cross-presented to CD8 T cells by CD8+ dendritic cells. *J. Immunol.* 166:5327–5330.

Pulendran, B., J.L. Smith, G. Caspary, K. Brasel, D. Pettit, E. Maraskovsky, and C.R. Maliszewski. 1999. Distinct dendritic cell subsets differentially regulate the class of immune response in vivo. *Proc. Natl. Acad. Sci. USA.* 96:1036–1041. doi:10.1073/pnas.96.3.1036

Radford, K.J., C.J. Turtle, A.J. Kassianos, and D.N. Hart. 2006. CD11c+ blood dendritic cells induce antigen-specific cytotoxic T lymphocytes with similar efficiency compared to monocyte-derived dendritic cells despite higher levels of MHC class I expression. *J. Immunother.* 29:596–605. doi:10.1097/01.cji.0000211310.90621.5d

Reis e Sousa, C., S. Hieny, T. Scharton-Kersten, D. Jankovic, H. Charest, R.N. Germain, and A. Sher. 1997. In vivo microbial stimulation induces rapid CD40 ligand-independent production of interleukin 12 by dendritic cells and their redistribution to T cell areas. *J. Exp. Med.* 186:1819–1829. doi:10.1084/jem.186.11.1819

Robbins, S.H., T. Walzer, D. Dembélé, C. Thibault, A. Defays, G. Bessou, H. Xu, E. Vivier, M. Sellars, P. Pierre, et al. 2008. Novel insights into the relationships between dendritic cell subsets in human and mouse revealed by genome-wide expression profiling. *Genome Biol.* 9:R17. doi:10.1186/gb-2008-9-1-r17

Rudd, B.D., E. Burstein, C.S. Duckett, X. Li, and N.W. Lukacs. 2005. Differential role for TLR3 in respiratory syncytial virus-induced chemokine expression. *J. Virol.* 79:3350–3357. doi:10.1128/JVI.79.6.3350-3357.2005

Sancho, D., D. Mourão-Sá, O.P. Joffre, O. Schulz, N.C. Rogers, D.J. Pennington, J.R. Carlyle, and C. Reis e Sousa. 2008. Tumor therapy in mice via antigen targeting to a novel, DC-restricted C-type lectin. *J. Clin. Invest.* 118:2098–2110. doi:10.1172/JCI34584

Sancho, D., O.P. Joffre, A.M. Keller, N.C. Rogers, D. Martínez, P. Hernanz-Falcón, I. Rosewell, and C. Reis e Sousa. 2009. Identification of a dendritic cell receptor that couples sensing of necrosis to immunity. *Nature.* 458:899–903. doi:10.1038/nature07750

Scheu, S., P. Dresing, and R.M. Locksley. 2008. Visualization of IFNbeta production by plasmacytoid versus conventional dendritic cells under specific stimulation conditions in vivo. *Proc. Natl. Acad. Sci. USA.* 105:20416–20421. doi:10.1073/pnas.0808537105

Schiavoni, G., F. Mattei, P. Sestili, P. Borghi, M. Venditti, H.C. Morse III, F. Belardelli, and L. Gabriele. 2002. ICSBP is essential for the development of mouse type I interferon-producing cells and for the generation and activation of CD8α^+ dendritic cells. *J. Exp. Med.* 196:1415–1425. doi:10.1084/jem.20021263

Schnorrer, P., G.M. Behrens, N.S. Wilson, J.L. Pooley, C.M. Smith, D. El-Sukkari, G. Davey, F. Kupresanin, M. Li, E. Maraskovsky, et al. 2006. The dominant role of CD8+ dendritic cells in cross-presentation is not dictated by antigen capture. *Proc. Natl. Acad. Sci. USA.* 103:10729–10734. doi:10.1073/pnas.0601956103

Schnurr, M., Q. Chen, A. Shin, W. Chen, T. Toy, C. Jenderek, S. Green, L. Miloradovic, D. Drane, I.D. Davis, et al. 2005. Tumor antigen processing and presentation depend critically on dendritic cell type and the mode of antigen delivery. *Blood.* 105:2465–2472. doi:10.1182/blood-2004-08-3105

Schulz, O., S.S. Diebold, M. Chen, T.I. Näslund, M.A. Nolte, L. Alexopoulou, Y.T. Azuma, R.A. Flavell, P. Liljeström, and C. Reis e Sousa. 2005. Toll-like receptor 3 promotes cross-priming to virus-infected cells. *Nature.* 433:887–892. doi:10.1038/nature03326

Shortman, K., and Y.J. Liu. 2002. Mouse and human dendritic cell subtypes. *Nat. Rev. Immunol.* 2:151–161. doi:10.1038/nri746

Skokos, D., and M.C. Nussenzweig. 2007. CD8⁻ DCs induce IL-12–independent Th1 differentiation through Delta 4 Notch–like ligand in response to bacterial LPS. *J. Exp. Med.* 204:1525–1531.

Soares, H., H. Waechter, N. Glaichenhaus, E. Mougneau, H. Yagita, O. Mizenina, D. Dudziak, M.C. Nussenzweig, and R.M. Steinman. 2007. A subset of dendritic cells induces CD4⁺ T cells to produce IFN-γ by an IL-12–independent but CD70-dependent mechanism in vivo. *J. Exp. Med.* 204:1095–1106. doi:10.1084/jem.20070176

Steinman, R.M. 2008. Dendritic cells in vivo: a key target for a new vaccine science. *Immunity*. 29:319–324. doi:10.1016/j.immuni.2008.08.001

Stoitzner, P., C.H. Tripp, A. Eberhart, K.M. Price, J.Y. Jung, L. Bursch, F. Ronchese, and N. Romani. 2006. Langerhans cells cross-present antigen derived from skin. *Proc. Natl. Acad. Sci. USA*. 103:7783–7788. doi:10.1073/pnas.0509307103

Urban, B.C., D. Cordery, M.J. Shafi, P.C. Bull, C.I. Newbold, T.N. Williams, and K. Marsh. 2006. The frequency of BDCA3-positive dendritic cells is increased in the peripheral circulation of Kenyan children with severe malaria. *Infect. Immun.* 74:6700–6706. doi:10.1128/IAI.00861-06

Velásquez-Lopera, M.M., L.A. Correa, and L.F. García. 2008. Human spleen contains different subsets of dendritic cells and regulatory T lymphocytes. *Clin. Exp. Immunol.* 154:107–114. doi:10.1111/j.1365-2249.2008.03734.x

Villadangos, J.A., and P. Schnorrer. 2007. Intrinsic and cooperative antigen-presenting functions of dendritic-cell subsets in vivo. *Nat. Rev. Immunol.* 7:543–555. doi:10.1038/nri2103

Vulink, A., K.J. Radford, C. Melief, and D.N. Hart. 2008. Dendritic cells in cancer immunotherapy. *Adv. Cancer Res.* 99:363–407. doi:10.1016/S0065-230X(07)99006-5

Wills, M.R., A.J. Carmichael, K. Mynard, X. Jin, M.P. Weekes, B. Plachter, and J.G. Sissons. 1996. The human cytotoxic T-lymphocyte (CTL) response to cytomegalovirus is dominated by structural protein pp65: frequency, specificity, and T-cell receptor usage of pp65-specific CTL. *J. Virol.* 70:7569–7579.